Electromagnetic wave propagation through a dielectric slab placed in a chiral medium using the transfer matrix technique

A. GHAFFAR[a,b], MAJEED A. S. ALKANHAL[a]
[a] *Department of Electrical Engineering, King Saud University, Saudi Arabia*
[b]*Department of Physics, University of Agriculture, Faisalabad, Pakistan*

A theoretical investigation of the interaction of electromagnetic waves with a dielectric slab placed in a chiral medium is presented. From the chiral medium either a left circularly polarized (LCP) wave or a right circularly polarized (RCP) wave is obliquely incident on the dielectric slab interface placed in the chiral medium. Two waves RCP and LCP are reflected into the chiral medium and one wave is transmitted into the slab at the first interface. Similarly, Two RCP and LCP waves are transmitted into chiral medium and one wave is reflected into the slab at the second interface. The reflection and transmission coefficients at the chiral-dielectric and the dielectric-chiral interfaces have been formulated and obtained analytically using the transfer matrix technique. Numerical results are presented to explain the effect of the chirality and the incidence angle on the reflection and transmission coefficients and, hence, on the reflected and the transmitted powers. The accuracy of the presented formulation and results has been validated by comparison with other results available in the literature.

(Received October 24, 2013; accepted May 05, 2014)

Keywords: Dielectric, Chiral, Right circularly polarized, Left circularly polarized

1. Introduction

Electromagnetics and microwave technology is moving ahead with great pace. One of the frontiers at which major conquests are being made is that of new electromagnetic materials like chiral media. In recent years, chiral materials have attained a lot of attention because of their synthetic realizability to have flexible properties such as negative refractive index [1-3]. These metamaterials, with their permittivity and permeability designed artificially from negative to positive values, may exhibit special electromagnetic response that is not expected in natural materials. These synthesized materials are suitable to be used in a variety of radio and microwave devices, such as weakly or strongly reflecting coatings and polarization converters [3]. In chiral materials, the tiny-size inclusions do not have a symmetry center. Usually, they are distributed uniformly and uncontrollably oriented in an isotropic mass medium. These types of media are considered isotropic and homogeneous. Such materials are birefringent since the electromagnetic field in such a medium consists of two components, namely, left circularly polarized and right circularly polarized eigenwave with different directions of rotation and different wave numbers [4].

Many researchers have studied the interaction of electromagnetic waves with chiral layers and their possible structures [5-11]. Reflection and transmission of waves at a dielectric-chiral interface have been studied by Silverman [12]. He derived the Fresnel amplitudes for specular reflection and refraction at the surface of the chiral medium. Lakhtakia et al. [13] have examined the microwave reflection characteristics of a planar achiral-chiral interface. Interaction of electromagnetic waves through a chiral slab is discussed by Bassiri et al. [14]. They presented an analytical solution to the transmitted and reflected waves for an incident wave of parallel polarization. Sabah and Uckun [15] presented the analysis of the plane wave in a multilayer chiral medium to determine the plane wave behavior in the multilayer chiral structure. The electromagnetic wave reflection and transmission properties at a chiral-dielectric interface were investigated, also, by Cory et al [16]. Sobia et al. studied the reflection and transmission of electromagnetic waves from a uniaxial chiral slab placed in an isotropic chiral medium [17].

The intense research in chiral materials has conjectured that the complex properties of these materials can find growing applications in the microwaves and higher frequency bands [18]. The study of electromagnetic waves through a dielectric slab placed in chiral medium could be of practical importance in remote sensing diagnosing, in the design of effective electromagnetic shields, or the in prediction of materials structural deformation.

In this paper we derived the reflection and transmission coefficients at a chiral-dielectric and dielectric-chiral interfaces by the transfer matrix

technique. The transfer matrix technique is effective for the analysis of the electromagnetic wave propagation [19,20] and here it will be applied to analyze the interaction of electromagnetic waves with an infinite dielectric slab placed in a chiral medium. The amplitudes of the waves to the left side of the slab are expressed in terms of those on the right side. This defines the transfer matrix **M**. In a two-dimensional system, the waves in both the left and the right sides of the slab have four components, two are moving to the right and two are moving to the left. Therefore, the transfer matrix **M** is a 4×4 matrix. The 4 ×4 scattering matrix **S** describes the outgoing waves in terms of the ingoing waves. The relationship between the transfer and the scattering matrices will be introduced. Through the transfer matrix formalism, the transmission and reflection coefficients can be easily defined and calculated. Once the transmission and reflection coefficients are derived, then the study of the material electromagnetic properties can be investigated. To validate the formulation presented in this paper, we also solved the problem using the method described in [14]. Both techniques give the same results which prove the accuracy of the presented formulations.

Analysis has been carried out for different values of chirality parameters of the chiral medium. Throughout this analysis, we have assumed that $\mu_t = \mu_z = \mu_0$ and $\frac{\omega}{2\pi} = 10\ GHz$. This analysis will reveal the nature of the generated waves inside the chiral medium as compared to the transmitted and reflected waves in achiral media. The effect of chirality on the polarization properties of the electromagnetic waves will be examined as well.

2. Electromagnetic fields in chiral medium

The Constitutive relations for electromagnetic (EM) fields in chiral medium involve the coupled nature of both electric and magnetic fields [1-5].

$$\boldsymbol{D} = \epsilon \boldsymbol{E} + i\gamma \boldsymbol{B} \tag{1}$$

$$\boldsymbol{H} = i\gamma \boldsymbol{E} + (1/\mu)\, \boldsymbol{B} \tag{2}$$

These relations are for time-harmonic fields when in a chiral medium. γ is the dimensionless chirality parameter of the material [18] and ϵ , μ are, respectively, are the permittivity and permeability of the chiral medium. Two distinct waves propagate in the chiral medium: a left circularly polarized wave (LCP) and a right circularly polarized wave (RCP) with the respective wave numbers

$$h_1 = \omega\mu\gamma + (\omega^2\mu^2\gamma^2 + k^2)^{1/2}$$

$$h_2 = -\omega\mu\gamma + (\omega^2\mu^2\gamma^2 + k^2)^{1/2}$$

where $k^2 = \omega^2 \varepsilon \mu$.

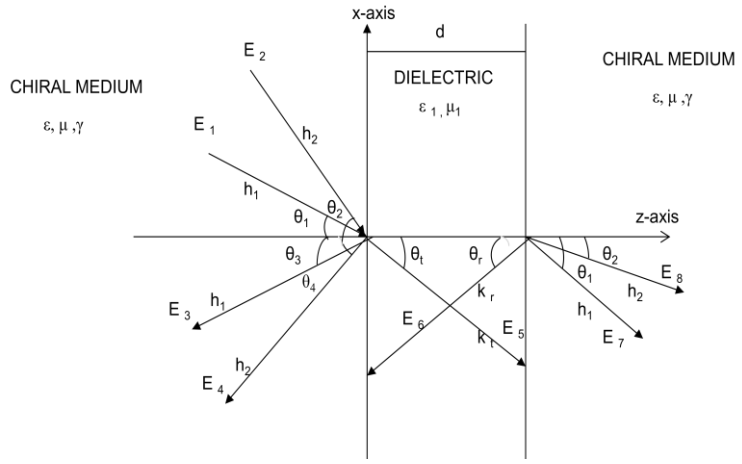

Fig. 1. Oblique incidence on an infinite dielectric slab placed in a chiral medium.

Consider a dielectric slab of uniform thickness d placed in a chiral medium as shown in Fig. 1. The dielectric slab $(\varepsilon_1\ , \mu_1)$ is confined between two infinitely extended planes, $z = 0$ and $z = d$, and lies between two chiral media with the same constitutive parameters (ε, μ). Suppose that $(\boldsymbol{E_1^c}, \boldsymbol{H_1^c})$ and $(\boldsymbol{E_2^c}, \boldsymbol{H_2^c})$ represent the incident right circularly polarized (RCP) wave and left circularly polarized (LCP) wave respectively. Similarly $(\boldsymbol{E_3^c}, \boldsymbol{H_3^c})$ and $(\boldsymbol{E_4^c}, \boldsymbol{H_4^c})$ represent the reflected right circularly polarized wave and left circularly polarized wave respectively. Either LCP or RCP plane waves is incident upon interface $z = 0$ from the zone $z \leq 0$.

The appropriate form to express the fields in zone $z \leq 0$ is represented by the following components [16]

$$\boldsymbol{E_1^c} = E_1^c\left(\cos\theta_1 \hat{\boldsymbol{e}}_x + \sin\theta_1 \hat{\boldsymbol{e}}_z + i\hat{\boldsymbol{e}}_y\right) e^{ih_1(z\cos\theta_1 - x\sin\theta_1)} \tag{3a}$$

$$\boldsymbol{H_2^c} = -i\mathrm{Z}^{-1}\boldsymbol{E_1^c} \tag{3b}$$

$$\boldsymbol{E_2^c} = E_2^c\left(\cos\theta_2 \hat{\boldsymbol{e}}_x + \sin\theta_1 \hat{\boldsymbol{e}}_z - i\hat{\boldsymbol{e}}_y\right) e^{ih_2(z\cos\theta_1 - x\sin\theta_1)} \tag{3c}$$

$$\boldsymbol{H_2^c} = -i\mathrm{Z}^{-1}\boldsymbol{E_2^c} \tag{3d}$$

$$\boldsymbol{E_3^c} = E_3^c\left(\sin\theta_1\hat{\boldsymbol{e}}_z - \cos\theta_1\hat{\boldsymbol{e}}_x + i\hat{\boldsymbol{e}}_y\right)\mathrm{e}^{-ih_1(z\cos\theta_1 + x\sin\theta_1)} \tag{3e}$$

$$\boldsymbol{H_3^c} = -i\mathrm{Z}^{-1}\boldsymbol{E_3^c} \tag{3f}$$

$$\boldsymbol{E_4^c} = E_4^c\left(\sin\theta_2\hat{\boldsymbol{e}}_z - \cos\theta_2\hat{\boldsymbol{e}}_x + i\hat{\boldsymbol{e}}_y\right)\mathrm{e}^{-ih_2(z\cos\theta_2 + x\sin\theta_2)} \tag{3g}$$

$$\boldsymbol{H_4^c} = -i\mathrm{Z}^{-1}\boldsymbol{E_4^c} \tag{3h}$$

where E_1^c and E_2^c represent the initial amplitudes of the incident waves, while E_3^c and E_4^c are the amplitudes of the reflected waves. θ_1 and θ_2 are the angles of incidence of the LCP and the RCP plane waves in the chiral medium.

It is assumed that ($\boldsymbol{E_5^d}$, $\boldsymbol{H_5^d}$) and ($\boldsymbol{E_6^d}$, $\boldsymbol{H_6^d}$) represent the transmitted wave at the first interface and the reflected wave from the second interface respectively. The appropriate form of these fields can be expressed by the following equations

$$\boldsymbol{E_5^d} = \left[iE_{t\perp}\hat{\boldsymbol{e}}_y + E_{t\parallel}(cos\theta_t\hat{\boldsymbol{e}}_x + sin\theta_t\hat{\boldsymbol{e}}_z)\right] \boldsymbol{e}^{ik_t(zcos\theta_t - x\,sin\theta_t)} \tag{4a}$$

$$\boldsymbol{H_5^d} = \sqrt{\frac{\mu}{\varepsilon}}\left[E_{t\parallel}\hat{\boldsymbol{e}}_y - iE_{t\perp}(cos\theta_t\hat{\boldsymbol{e}}_x + \ sin\theta_t\hat{\boldsymbol{e}}_z)\right] \boldsymbol{e}^{ik_t(zcos\theta_t - x\,sin\theta_t)} \tag{4b}$$

$$\boldsymbol{E_6^d} = [iE_{r\perp}\,\hat{\boldsymbol{e}}_y + E_{r\parallel}(sin\theta_r\hat{\boldsymbol{e}}_z - \ cos\theta_r\hat{\boldsymbol{e}}_x)] \boldsymbol{e}^{ik_t(zcos\theta_r - x\,sin\theta_r)} \tag{4c}$$

$$\boldsymbol{H_6^d} = \sqrt{\frac{\mu_0}{\varepsilon_0}}\left[iE_{r\perp}\,\hat{\boldsymbol{e}}_y + E_{r\parallel}(sin\theta_r\hat{\boldsymbol{e}}_z - \ cos\theta_r\hat{\boldsymbol{e}}_x)\right] \boldsymbol{e}^{ik_t(zcos\theta_r - x\,sin\theta_r)} \tag{4d}$$

In these equations $E_{t\perp}, E_{t\parallel}$ are amplitudes of the transmitted fields at the first interface and $E_{r\perp}, E_{r\parallel}$ are amplitudes of the reflected fields at the second interface. θ_t is the angle of refraction from the first interface and θ_r is the angle of refraction of the LCP and RCP polarized waves at the second interface, and $k^2 = \omega^2\varepsilon_1\mu_1$ with ε_1 , μ_1 are permittivity and permeability of dielectric slab, respectively. Suppose that ($\boldsymbol{E_7^c}$, $\boldsymbol{H_7^c}$) and ($\boldsymbol{E_8^c}$, $\boldsymbol{H_8^c}$) represent, respectively, the right circularly polarized (RCP) wave and the left circularly polarized(LCP) wave transmitted from the dielectric slab to the chrial medium at the second interface expressed as [14]

$$\boldsymbol{E_7^c} = E_7^c\left(\cos\theta_1\hat{\boldsymbol{e}}_x + \sin\theta_1\hat{\boldsymbol{e}}_z + i\hat{\boldsymbol{e}}_y\right)\mathrm{e}^{ih_1(z\cos\theta_1 - x\sin\theta_1)} \tag{5a}$$

$$\boldsymbol{H_7^c} = -i\mathrm{Z}^{-1}\boldsymbol{E_7^c} \tag{5b}$$

$$\boldsymbol{E_8^c} = E_8^c\left(\cos\theta_2\hat{\boldsymbol{e}}_x + \sin\theta_1\hat{\boldsymbol{e}}_z - i\hat{\boldsymbol{e}}_y\right)\mathrm{e}^{ih_2(z\cos\theta_2 - x\sin\theta_2)} \tag{5c}$$

$$\boldsymbol{H_8^c} = -i\mathrm{Z}^{-1}\boldsymbol{E_7^c} \tag{5d}$$

3. Derivation of reflection and transmission coefficient using the transfer matrix technique

By imposing the continuity of the tangential components of the electric and magnetic fields at the interfaces, both in phase and in magnitude, the transmission and the reflection coefficients at each interface can be found. From the boundary condition at the interface, it is inferred that [7]

$$h_1Sin\theta_1 = h_2Sin\theta_2 = h_1Sin\theta_3 = h_2Sin\theta_4 = k_tSin\theta_t = k_rSin\theta_r \tag{6}$$

Eq. (6) is Snell's law which relates the incidence, reflection and transmission angles. After applying the boundary conditions at the interfaces with the use of Eq. (6), the relationships among the fields in all regions can be expressed by the transfer matrices. The boundary conditions at the first interface give the transfer matrix **M** as

$$\begin{bmatrix} E_1^c \\ E_2^c \\ E_3^c \\ E_4^c \end{bmatrix} = \mathbf{M} \begin{bmatrix} E_{t\parallel} \\ E_{t\perp} \\ E_{r\parallel} \\ E_{r\perp} \end{bmatrix} \tag{7}$$

where **M** is a 4×4 transfer matrix which may be defined as

$$M = AB$$

In the above equation, matrices A and B are given by

$$\boldsymbol{A} = \begin{bmatrix} 1 & -1 & 1 & -1 \\ \cos\theta_1 & \cos\theta_2 & -\cos\theta_1 & -\cos\theta_2 \\ Z^{-1} & Z^{-1} & Z^{-1} & Z^{-1} \\ Z^{-1}\cos\theta_1 & -Z^{-1}\cos\theta_2 & -Z^{-1}\cos\theta_1 & Z^{-1}\cos\theta_2 \end{bmatrix}^{-1}$$

$$\boldsymbol{B} = \begin{bmatrix} 0 & 1 & 0 & 1 \\ \cos\theta_3 & 0 & \cos\theta_3 & 0 \\ \eta^{-1} & 0 & \eta^{-1} & 0 \\ 0 & \eta^{-1}cos\theta_3 & 0 & \eta^{-1}cos\theta_3 \end{bmatrix}$$

The boundary conditions at the second interface give the scattering matrix S where

$$\begin{bmatrix} E_{t\parallel} \\ E_{t\perp} \\ E_{r\parallel} \\ E_{r\perp} \end{bmatrix} = \mathrm{S} \begin{bmatrix} E_7^c \\ E_8^c \end{bmatrix} \tag{8}$$

and S is a 4×4 transfer matrix defined as

$$S = CD \tag{9}$$

In the above equation, matrices C and D are given by

$$\boldsymbol{C}=\begin{bmatrix} 0 & e^{-ik_1 dcos\theta_3} & -e^{ih_1 dcos\theta_1} & e^{ih_2 dcos\theta_2} \\ cos\theta_3 e^{-ik_1 dcos\theta_3} & 0 & cos\theta_1 e^{ih_1 dcos\theta_1} & cos\theta_2 e^{ih_2 dcos\theta_2} \\ \eta^{-1} e^{-ik_1 dcos\theta_3} & 0 & -Z^{-1} e^{ih_1 dcos\theta_1} & -Z^{-1} e^{ih_2 dcos\theta_2} \\ 0 & -\eta^{-1} cos\theta_3 e^{-ik_1 dcos\theta_3} & -Z^{-1} cos\theta_1 e^{ih_1 dcos\theta_1} & Z^{-1} cos\theta_2 e^{ih_2 dcos\theta_2} \end{bmatrix}^{-1}$$

$$\boldsymbol{D}=\begin{bmatrix} -e^{ih_1 dcos\theta_1} & e^{ih_2 dcos\theta_2} \\ cos\theta_1 e^{ih_1 dcos\theta_1} & cos\theta_2 e^{ih_2 dcos\theta_2} \\ -Z^{-1} e^{ih_1 dcos\theta_1} & -Z^{-1} e^{ih_2 dcos\theta_2} \\ -Z^{-1} cos\theta_1 e^{ih_1 dcos\theta_1} & Z^{-1} cos\theta_2 e^{ih_2 dcos\theta_2} \end{bmatrix}$$

From above equations, we can get the reflection and the transmission coefficients in case of oblique incidence in the following form

$$\begin{pmatrix} E_3^c \\ E_4^c \end{pmatrix} = \begin{pmatrix} R_{11} & R_{12} \\ R_{21} & R_{22} \end{pmatrix} \begin{pmatrix} E_1^c \\ E_2^c \end{pmatrix} \quad (10)$$

$$\begin{pmatrix} E_7^c \\ E_8^c \end{pmatrix} = \begin{pmatrix} T_{11} & T_{12} \\ T_{21} & T_{22} \end{pmatrix} \begin{pmatrix} E_1^c \\ E_2^c \end{pmatrix} \quad (11)$$

The expressions of the elements in matrices of equations (10) and (11) are omitted for simplification.

4 Computing the reflection and transmission coefficients

The boundary conditions of the Electromagnetic fields at interfaces $x = 0,\ z = 0$ and $x = 0, z = d$ state that

$$(\boldsymbol{E_1^c} + \boldsymbol{E_2^c} + \boldsymbol{E_3^c} + \boldsymbol{E_4^c}) \times \hat{e}_z = (\boldsymbol{E_5^d} + \boldsymbol{E_6^d}) \times \hat{e}_z \quad (12)$$

$$(\boldsymbol{H_1^c} + \boldsymbol{H_2^c} + \boldsymbol{H_3^c} + \boldsymbol{H_4^c}) \times \hat{e}_z = (\boldsymbol{H_5^d} + \boldsymbol{H_6^d}) \times \hat{e}_z \quad (13)$$

$$(\boldsymbol{E_5^d} + \boldsymbol{E_6^d}) \times \hat{e}_z = (\boldsymbol{E_7^c} + \boldsymbol{E_8^c}) \times \hat{e}_z \quad (14)$$

$$(\boldsymbol{H_5^d} + \boldsymbol{H_6^d}) \times \hat{e}_z = (\boldsymbol{H_7^c} + \boldsymbol{H_8^c}) \times \hat{e}_z \quad (15)$$

A system of eight inhomogeneous equations with eight unknowns, $E_3^c,\ E_4^c, E_{t\parallel}, E_{t\perp}, E_{r\parallel}, E_{r\perp}, E_7^c$ and E_8^c is obtained. This system of equations can be written in the following matrix form:

$$\begin{bmatrix} E_3^c \\ E_4^c \\ E_{t\parallel} \\ E_{t\perp} \\ E_{r\parallel} \\ E_{r\perp} \\ E_7^c \\ E_8^c \end{bmatrix} = Y^{-1} \begin{bmatrix} E_1^c - E_2^c \\ \cos\theta_1 E_1^c + \cos\theta_2 E_2^c \\ Z^{-1} E_1^c + Z^{-1} E_2^c \\ Z^{-1}(\cos\theta_1 E_1^c - \cos\theta_1 E_2^c) \\ 0 \\ 0 \\ 0 \\ 0 \end{bmatrix}$$

$$X = Y^{-1} Z \quad (16)$$

where

$$Y = \begin{bmatrix} -1 & 1 & 0 & 1 & 1 & 0 & 0 & 0 \\ cos\theta_1 & cos\theta_2 & cos\theta_3 & 0 & 0 & cos\theta_3 & 0 & 0 \\ -\frac{1}{Z} & -\frac{1}{Z} & \frac{1}{\eta} & 0 & 0 & \frac{i}{\eta} & 0 & 0 \\ \frac{cos\theta_1}{Z} & -\frac{cos\theta_2}{Z} & 0 & \frac{cos\theta_3}{\eta} & \frac{cos\theta_3}{\eta} & 0 & 0 & 0 \\ 0 & 0 & 0 & e^{ik1dcos\theta_3} & e^{-ik1dcos\theta_3} & 0 & -e^{ih1dcos\theta_1} & e^{ih2dcos\theta_2} \\ 0 & 0 & -cos\theta_3\, e^{ik1dcos\theta_3} & 0 & 0 & cos\theta_3\, e^{-ik1dcos\theta_3} & cos\theta_1 e^{ih1dcos\theta_1} & cos\theta_2 e^{ih2dcos\theta_2} \\ 0 & 0 & \frac{1}{\eta} e^{ik1dcos\theta_3} & 0 & 0 & \frac{i}{\eta} e^{-ik1dcos\theta_3} & -\frac{e^{ih1dcos\theta_1}}{Z} & -\frac{e^{ih2dcos\theta_2}}{Z} \\ 0 & 0 & 0 & \frac{cos\theta_3}{\eta} e^{ik1dcos\theta_3} & -\frac{cos\theta_3}{\eta} e^{-ik1dcos\theta_3} & 0 & -\frac{icos\theta_1 e^{ih1dcos\theta_1}}{Z} & \frac{icos\theta_2 e^{ikdcos\theta_2}}{Z} \end{bmatrix}$$

$$X = \begin{bmatrix} E_3^c \\ E_4^c \\ E_{t\parallel} \\ E_{t\perp} \\ E_{r\parallel} \\ E_{r\perp} \\ E_7^c \\ E_8^c \end{bmatrix} \quad \text{And} \quad Z = \begin{bmatrix} E_1^c - E_2^c \\ \cos\theta_1 E_1^c + \cos\theta_2 E_2^c \\ Z^{-1} E_1^c + Z^{-1} E_2^c \\ Z^{-1}(\cos\theta_1 E_1^c - \cos\theta_1 E_2^c) \\ 0 \\ 0 \\ 0 \\ 0 \end{bmatrix}$$

where $Z = \sqrt{\frac{\mu}{\varepsilon}}\left(1 + \frac{\mu}{\varepsilon}{\gamma_1}^2\right)^{-\frac{1}{2}}$

The inversion of the Y matrix can be carried out numerically. The numerical solution of equation (16), enables the direct computations of the transmitted and the reflected field components in the dielectric slab and the host chiral medium.

5. Numerical results and discussions

In this section, the above procedure is utilized to investigate the electromagnetic properties of the dielectric slab of thickness d placed in the chiral medium when the incident fields from the chiral medium is a right circularly

polarized or a right circularly polarized plane wave. To check the accuracy of the formulation and the derived expressions by the transfer matrix technique, the problem is, additionally, solved by another technique given in literature [14]. Both techniques give exactly the same results. The transmission and reflection coefficients are calculated as a function of the incidence angle θ_2 varying from 0 to 90^0 (degrees). It is assumed that $\mu = \mu_0, \epsilon = 4\,\epsilon_0$ and $\frac{\omega}{2\pi} = 10\,GHz$ throughout these computations. The magnitude of the reflection coefficients as a function of the incidence angle θ_2 at $\gamma = 0.0001$ (solid line), $\gamma = 0.001$ (dotted line), $\gamma = 0.01$ (large dashed line), and $\gamma = 0.1$ (thick solid line) are shown in Fig. 2 to Fig. 5. The dielectric slab is of thickness $d = 5mm$ confined between two chiral media of the same constituents. It is found that the magnitude of the coefficient R_{11} increases as the incidence angle increases. It is also observed that with the increase in the chirality value, R_{11} decreases at lower angle of incidence but increases at greater values of the angle of incidence. The magnitude of the reflection coefficient R_{12} decreases with the increase in the angle of incidence and the increase in chirality causes increase in values of R_{12}. The Brewster angle appears at $\theta_2 = 76^0$ when the value of chirality parameter is 0.001. It is depicted that the increase in the angle of incidence and the value of chirality cause increase in the intensity of R_{21}. In Fig. 5 the reflection coefficient R_{22} is plotted versus the angle of incidence and the value of chirality. In this case the Brewster angle appears at $\theta_2 = 65^0$ when value of chirality parameter is 0.01. The magnitude of various transmission coefficients as a function of the incidence angle θ_2 at $\gamma = 0.0001$ (solid line), $\gamma = 0.001$ (dotted line), $\gamma = 0.01$ (large dashed line), and $\gamma = 0.1$ (thick solid) are shown in Fig. 6 to Fig. 9.

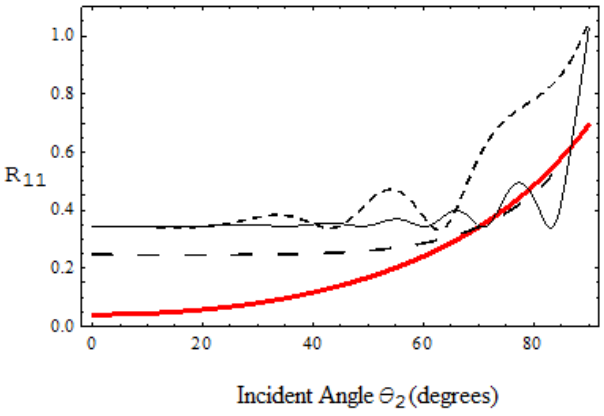

Fig. 2. The reflection coefficient R_{11} versus the angle of incidence θ_2 at $\gamma = 0.0001$ (solid line), $\gamma = 0.001$ (dotted line), $\gamma = 0.01$ (large dashed line) and $\gamma = 0.1$ (thick line).

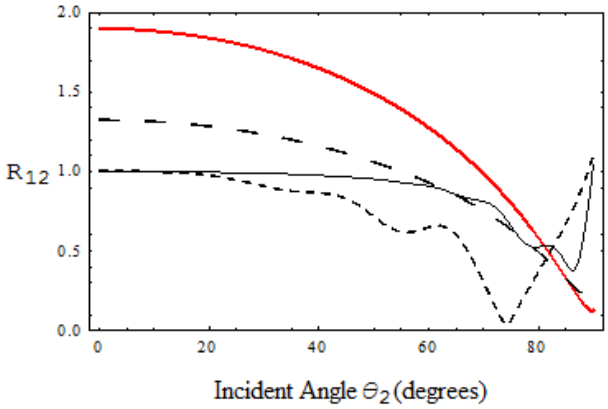

Fig. 3. The reflection coefficient R_{12} versus the angle of incidence θ_2 at $\gamma = 0.0001$ (solid l ine), $\gamma = 0.001$ (dotted line), $\gamma = 0.01$ (large dashed line) and $\gamma = 0.1$ (thick line).

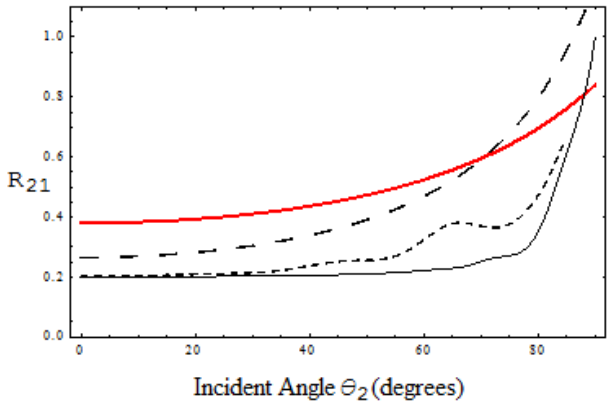

Fig. 4. The reflection coefficient R_{21} versus the angle of incidence θ_2 at $\gamma = 0.0001$ (solid line), $\gamma = 0.001$ (dotted line), $\gamma = 0.01$ (large dashed line), and $\gamma = 0.1$(thick line).

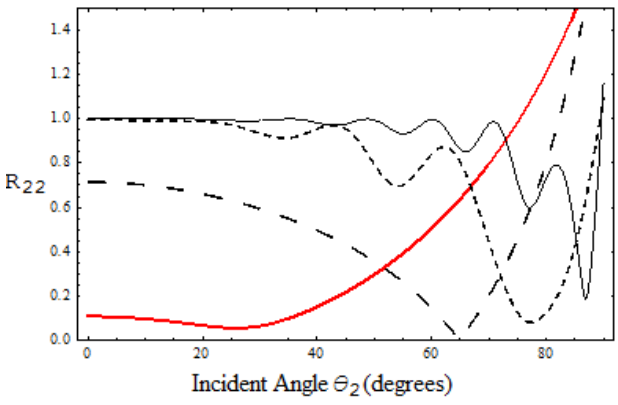

Fig. 5. The reflection coefficient R_{22} versus the angle of incidence θ_2 at $\gamma = 0.0001$ (solid l ine), $\gamma = 0.001$ (dotted line), $\gamma = 0.01$ (large dashed line), and $\gamma = 0.1$ (thick line).

The increase in the value of chirality parameter reduces the number of lobes in all components of the transmission coefficients. It is found that the magnitudes of the copolarized reflection coefficients T_{11}, T_{21} increase

as the incidence angle increases or the chirality parameter increases. At $\gamma = 0.01$ (large dashed line), the magnitude of the copolarized reflection coefficients T_{11}, T_{21} increases as the incidence angle increases. The cross polarized transmission coefficient T_{12} attains maximum magnitude at normal incidence and decreases with the increase of the incidence angle and becomes zero at $\theta_2 = 90^o$. The normalized reflected and transmitted power densities versus the angle of incidence θ_2 for different values of the chirality parameters at $\gamma = 0.0001$ (solid line), $\gamma = 0.001$ (dotted line), $\gamma = 0.01$ (large dashed line), and $\gamma = 0.1$ (thick solid line) are shown in Figures 10 and 11. It is found from calculations that the reflected power decreases as the incidence angle increases till $\theta_2 = 75^o$. At this angle of incidence, with the chirality parameter $\gamma = 0.001$, the Brewster angle achieved. The reflected power begin to increase after $\theta_2 = 75^o$ and reaches a maximum value at $\theta_2 = 90^o$. Fig. 11 shows that the normalized transmitted power increase as the incidence angle increases till $\theta_2 = 75^o$. The transmitted power begins to decrease after $\theta_2 = 75^o$ and gives a minimum value at $\theta_2 = 90^o$ as expected.

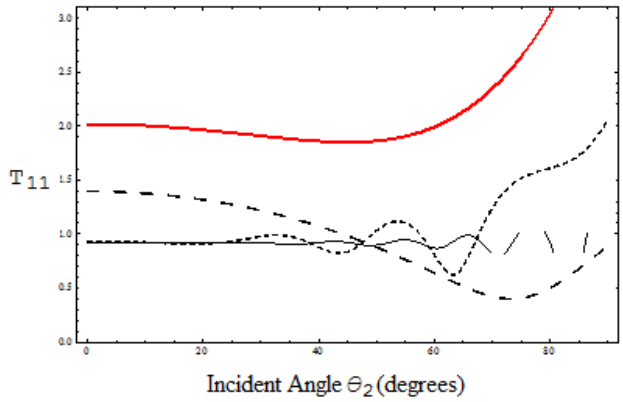

Fig. 6. The transmission coefficient T_{11} versus the angle of incidence θ_2 at $\gamma = 0.0001$ (solid line), $\gamma = 0.001$ (dotted line), $\gamma = 0.01$ (large dashed line), and $\gamma = 0.1$(thick line).

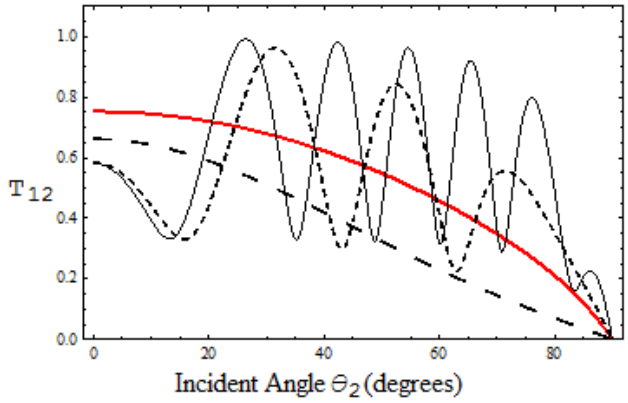

Fig. 7. The transmission coefficient T_{12} versus the angle of incidence θ_2 at $\gamma = 0.0001$ (solid line), $\gamma = 0.001$ (dotted line), $\gamma = 0.01$ (large dashed line), and $\gamma = 0.1$ (thick line).

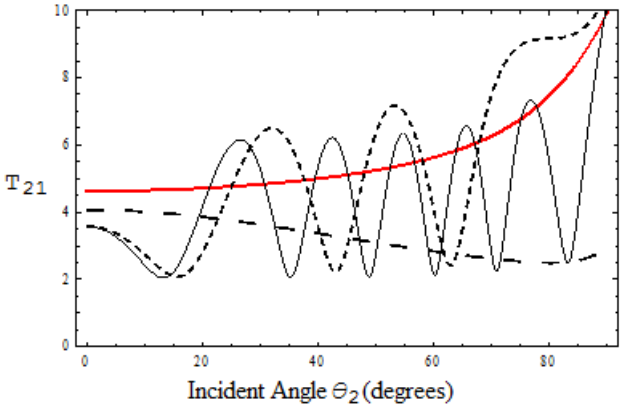

Fig. 8. The transmission coefficient T_{21} versus the angle of incidence θ_2 at $\gamma = 0.0001$ (solid line), $\gamma = 0.001$ (dotted line), $\gamma = 0.01$(large dashed line), and $\gamma = 0.1$(thick line).

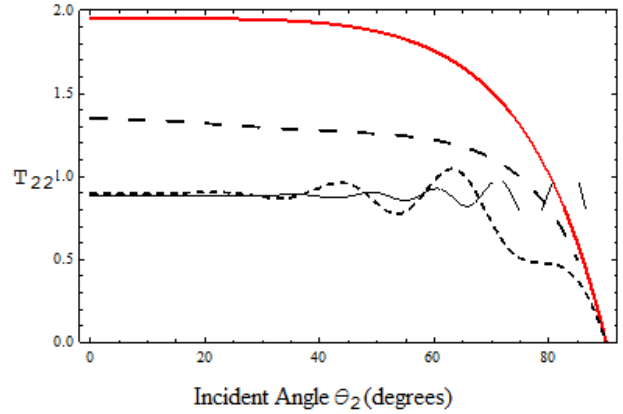

Fig. 9. The transmission coefficient T_{22} versus the angle of incidence θ_2 at $\gamma = 0.0001$ (solid line), $\gamma = 0.001$ (dotted line), $\gamma = 0.01$ (large dashed line), and $\gamma = 0.1$(thick line).

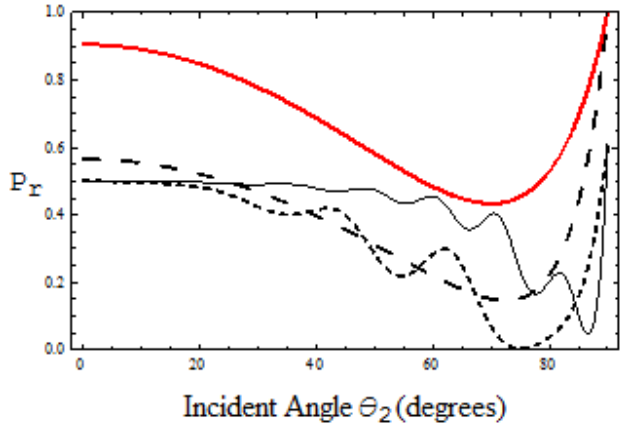

Fig. 10. The comparison of reflected power P_r versus the angle of incidence θ_2 at $\gamma = 0.0001$(solid line), $\gamma = 0.001$ (dot line) ,$\gamma = 0.01$ (large dashed line), and $\gamma = 0.1$(thick line)

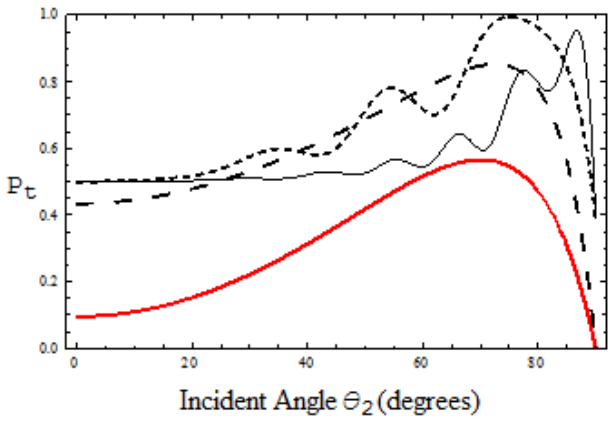

Fig. 11. The Comparison of reflected power P_t versus the angle of incidenceθ_2 at $\gamma = 0.0001$(solid line),$\gamma = 0.001$ (dot line) ,$\gamma = 0.01$ (large dashed line), and $\gamma = 0.1$(thick line).

6. Conclusion

In this research, the electromagnetic property of a dielectric slab placed in a chiral medium is studied using the transfer matrix technique. Mathematical formulation and analysis as well as numerical results for the reflection and transmission coefficients are presented as functions of the parameters of the dielectric slab and the host chiral media so that the behavior of wave propagation from chiral medium to dielectric medium and from dielectric medium to medium can be thoughtfully investigated. The effects of changes in the chirality parameter and the angle of incidence have been computed. From these results, it is concluded that the strength of the reflected copplarized components increase while the strength of reflected cross polarized components decrease with the increase of the chirality parameter of host medium. It is also observed that strength of the transmission coefficients increase with the increase of the chirality parameter of host medium. Formulation, analysis, and results presented in this work should be of potential applications for the design of microwave and optical devices such as polarization transformers.

Acknowledgment: The authors would like to thank the Deanship of the Scientific Research and the Research Centre at the College of Engineering, King Saud University, for the financial and administrative support.

References

[1] A. Lakhtakia, Beltrami Fields in chiral media, World Scientific, Singapore, 1994.
[2] I. V. Lindell, A. H. Sihvola, S. A. Tretyakov, A. J. Viitanen, Electromagnetic Waves in Chiral and Bi-Isotropic Media, Ch. 8, Artech House, Boston, London, 1994.
[3] I. V. Semchenko, S. A. Khakhomov, S. A. Tretyakov, A. H. Sihvola, Electromagnetics **21**, 401 (2001).
[4] X. M. Yang, T. Jun, Q. Cheng, IEEE Transaction on Antenna and Propagation, **55**, 2754 (2007).
[5] J. F. Dong, J. Li, Progress In Electromagnetics Research, **127**, 389 (2012).
[6] V. V. Fisanov, Radiofizika, **48**, 537 (2005).
[7] C. Sabah, G. G. Ögücü, S. Uckun, J. Optoelectron Adv. Mater., **8**, 1925 (2006).
[8] A. Ghaffar, M. Arif, Q. A. Naqvi, Majeed Alkanhal, Optik- Int. J. of Light and Electron Optics, **125**, 1589 (2014).
[9] A. Ghaffar, S. I. Ahmad, R. Fazal, S. Shukrullah, Q. A. Naqvi, Optik- Int. J. of Light and Electron Optics, **124**, 4947 (2013).
[10] A. Ghaffar, H. M. Shahbaz, Q. A. Naqvi, Int. J. of Applied Electromagnetics and Mechanics, **42**, 613 (2013).
[11] C. Sabah, G. G. Ögücü, S. Uckun, J. Optoelectron. Adv. Mater. **8**, 1918 (2006).
[12] M. P. Silverman, Journal of Optical Society America, A **3**, 830 (1986).
[13] A. Lakhtakia, V. V. Varadan, V. K. Varadan, Optical Society of America, **6**, 23 (1989).
[14] S. Bassiri, C. H. Papas, N. Engheta, Journal of Optical Society of America, A **5**, 1450 (1988).
[15] C. Sabah, S. Uckun, Science in China Series E: Technological Sciences, **49**, 457 (2006).
[16] H. Cory, I. Rosenhouse, Journal of Modern Optics, **38**, 1229 (1991).
[17] S. Shoukat, A. A. Syed, Q. A. Naqvi, International Journal of Applied Electromagnetics and Mechanics, **42**, 639 (2013).
[18] W. Bingnan, J. Zhou, T. Koschny, M. Kafesaki, C. M. Soukoulis, Journal of Optics, A**11,** 114003 (2009).
[19] P. M. Bell, J. B. Pendry, NATO ASI Series, **315**, 203 (1996).
[20] C. Charalambos, Katsidis, D. I. Siapkas, Applied Optics, **41**, 3978 (2002).

*Corresponding author: chabdulghaffar@yahoo.com
majeed@ksu.edu.sa